THE IMPACT OF AMORPHOUS-CRYSTALLINE CONTENT IN THE HYDRATION KINETICS OF A MODIFIED-BOF SLAG

Pavel Leonardo LOPEZ GONZALEZ, Bart BLANPAIN, Yiannis PONTIKES

KU Leuven, Department of Materials Engineering, 3001 Leuven, Belgium

pavelleonardo.lopezgonzalez@kuleuven.be, bart.blanpain@kuleuven.be, yiannis.pontikes@kuleuven.be

Introduction

The granulation of modified basic-oxygen-furnace slag (BOFS) provides mineralogical modifications that impact the slag reactivity.[1] The key is the particle size distribution generated during the granulation. When the stream is broken into droplets of variable size, differences in the actual cooling are generated. The effect can be traced after granulation by the estimation of the amorphous and crystalline contents present in the solidified particles. The present study quantifies the differences in the kinetics, the crystalline hydration products, and the early strength of binders produced using different size fractions of the granulated BOFS.

Materials and Methods

The modified BOFS (addition of about 13 wt% Al_2O_3) was produced at a pilot plant through water granulation.[1] The BOFS was sieved into three size fractions, as seen in Figure 1a), below 1.0 mm (F1), 1.6 to 1.0 mm (F2), and above 1.6 mm (F3). Fractions were milled to provide similar fineness of 4000 cm^2/g (± 5%). The quantified mineralogy has been previously reported[2] and is presented in Figure 1b.

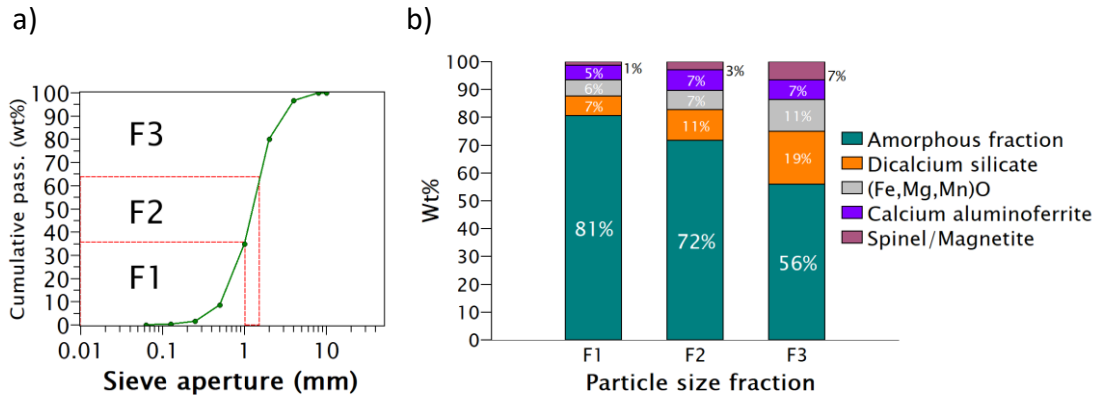

Figure 1: a) BOFS particle size distribution, the sieve apertures (1.0 and 1.6 mm) used to split into three size fractions is indicated; b) Quantified mineralogy of BOFS fractions[2]

Paste samples were produced by mixing the slags with water (water to slag mass ratio of 0.4). To track the reaction kinetics by means of heat flow and total heat evolution data, the samples were analysed using isothermal calorimetry with in-situ admix ampoules in a TAM Air calorimeter for 72 h. The reaction products developed within the first 2 h were identified using in-situ XRD. Patterns were collected every five minutes with a D2 Phaser (Bruker) measuring 2θ angles from 5° to 35°, with a step size of 0.02° and 0.6 s per step employing a Cu tube at a voltage of 30 kV and a current of 10 mA. The infrared spectra were acquired for wavelengths ranging from 400 until 1400 cm^{-1} using a Fourier transform infrared spectrometer model Alpha-P (Bruker) coupled with an attenuated total reflectance module (ATR-FTIR). Cubic specimens (20 mm side) were tested for compressive strength after 7 d.

Results

The isothermal calorimetry results are presented in Figure 2. Significant heat release occurred within the first 24 h for all fractions. For F1 and F2, the main heat flow curve presented three distinct stages with the main peak occurring after 8 h. In contrast, F3 heat flow was unimodal with a single peak appearing after 4 h. The total heat released by all fractions was similar after 72 h (333 J/g for F1, and 322 J/g for F2 and F3).

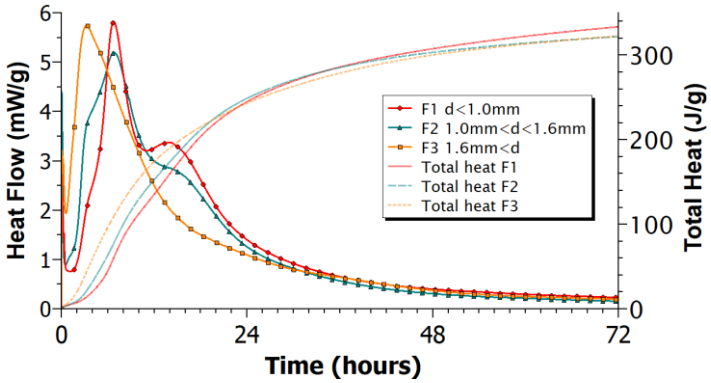

Figure 2: Heat flow and total heat released by the hydrated size fractions, W/S = 0.4

The XRD results in Figure 3 show that the intensity of the corresponding peaks increased with the crystalline content, being the highest for F3. For all fractions, the generation of $C_2(A,F)H_8$ and $C_4(A,F)H_x$, linked to C_4AF hydration,[3] was noticeable after 10 minutes. After 40 to 50 minutes, katoite $(Ca_3Al_2(SiO_4)_{3-x}(OH)_{4x}$ with x = 1.5-3) was identified in F1, strätlingite ($Ca_2Al_2SiO_7{\cdot}8H_2O$) in F3, and both types in F2.

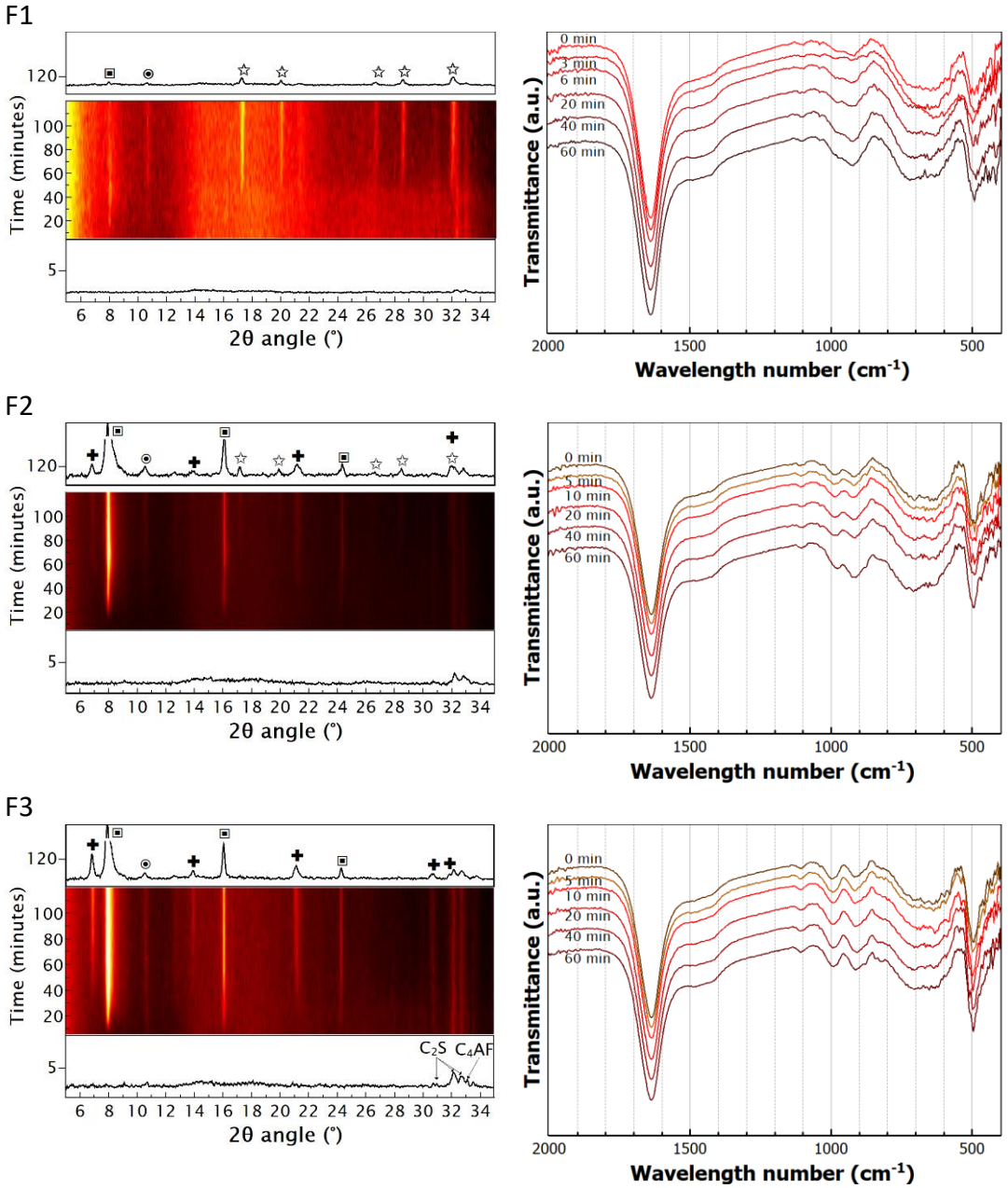

Figure 3: Left: in-situ XRD for the first 2 h of hydration of slag fractions (Cross- strätlingite; square – $C_2(A,F)H_8$; circle-$C_4(A,F)H_x$; star – katoite); brighter colour indicates sharper features; Right: Infrared spectra of fractions during the initial 60 minutes of hydration

The infrared spectra are presented in Figure 3. The features at time 0 were consistent with the presence of unreacted C_2S (500, 515, and 845 cm^{-1}), and calcium-aluminium rich phases (894, 900 to 980 cm^{-1}).[4] The peak between 1600 to 1700 cm^{-1} is associated with OH bending.[3] The only distinguishable change during early hydration was the increase of the peak at 925 cm^{-1} in F1 and F2 samples, which is compatible with the formation of katoite.[5] In Figure 4, the compressive strength after 7 d is presented. F3

developed 17.5 MPa on average and is higher than the values obtained for F1 and F2 (12.2 and 13.0 MPa respectively).

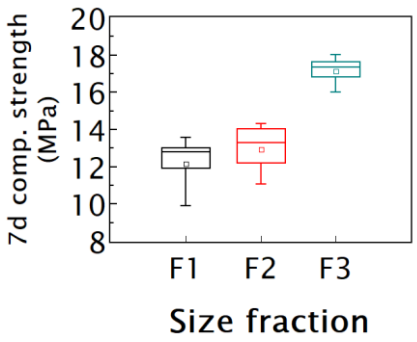

Figure 4: Compressive strength after 7 d of pastes produced using BOFS fractions

Conclusions

The granulation of modified BOFS produced differences in mineralogy that impacted the kinetics of hydration and the strength developed by paste specimens after 7 d. During the first 24 h of hydration, the heat released by F3 and F2 was faster than that of F1, which can be linked to the number of hydraulic phases available to react. AFm and hydrogarnet (katoite) were identified in all hydrated fractions. When tracking the first 2 h, AFm phases appeared after 10 and 40 min, which confirmed the presence of the fast-reacting calcium-aluminoferrite phases. The formation of katoite can be explained as the conversion of the initial hydration products into more stable forms. However, the presence of katoite in F1, where amounts of AFm phases were low, indicates that its formation might also be related to the dissolution of the amorphous fraction (currently under investigation). The differences in the strength developed are a direct consequence of the kinetics. The strength of F3 was 35% and 43% higher than those of F2 and F1, respectively. These findings support the use of selective particle size as a tool to control the mineralogy and early strength of BOFS binders.

References

1. P.L. Lopez Gonzalez, R.M. Novais, J.A. Labrincha, B. Blanpain, Y. Pontikes, “Modifications of basic-oxygen-furnace slag microstructure and their effect on the rheology and the strength of alkali-activated binders”, *Cem Concr Compos,* **97** 143-153 (2019).
2. P.L. Lopez Gonzalez, Y. Pontikes, “Microstructural tailoring of BOF steel slag for construction applications: amorphous content and its impact on reactivity and mechanical strength after alkali activation”, in *Proceedings 7th International Conference on Engineering of Waste and Biomass Valorisation (WasteEng18)*, edited by P.S. A. Nzihou, IMT Mines Albi, France, 2018.
3. H.F.W. Taylor, *Cement chemistry*, 2nd ed., Telford Publ, London, 2003.
4. S.N. Ghosh, S.K. Handoo, “Infrared and Raman spectral studies in cement and concrete (review)”, *Cem Concr Res,* **10** 771-782 (1980).
5. N.V. Chukanov, A.D. Chervonnyi, *Infrared Spectroscopy of Minerals and Related Compounds*, Springer International Publishing, Cham, 2016.